HHS Public Access

Author manuscript

J Neural Eng. Author manuscript; available in PMC 2015 June 17.

Published in final edited form as:

J Neural Eng. 2013 February ; 10(1): 016011. doi:10.1088/1741-2560/10/1/016011.

Preventing Neuronal Damage and Inflammation In-Vivo During Cortical Microelectrode Implantation Through the Use of Poloxamer P-188

A Misra[1], **P Kondaveeti**[1], **J Nissanov**[2], **K Barbee**[1], **P Shewokis**[1,3], **L Rioux**[2], and **KA Moxon**[1]

[1]Drexel University College of Biomedical Engineering

[2]Touro University Nevada, Department of Basic Sciences, College of Osteopathic Medicine

[3]Drexel University College of Nursing and Rehabilitation Sciences

Abstract

Objective—Test the efficacy of Poloxamer P188 to reduce cell death & immune response associated with mechanical trauma to cells during implantation of a chronic recording electrode.

Approach—Ceramic multi-site recording electrodes were implanted bilaterally into 15 adult male Long Evans rats. One of each pair was randomly assigned to receive a coating of Poloxamer while the other was treated with saline. The extent of neuron loss, and glial cell recruitment was characterized at 2, 4 and 6 weeks post implantation by stereologic analysis.

Main Result—At 2 and 4 weeks post implantation, Poloxamer coated implants showed significantly fewer glial cells and more neurons in the peri-electrode space than controls; however this significance was lost by 6 weeks.

Significance—These findings are the first tosuggest that Poloxamer has neuroprotective effects in-vivo, however at a fixed loading dose, these effects are limited to approximately 1 month post implantation.

1. Introduction

In recent years, a variety of brain machine interfaces (BMIs) have been proposed to help patients suffering from traumatic brain injury. Technologies including electroencephalography (EEG), intracranial microelectrodes, and functional imaging have been implemented to interface with the brain and attempt to restore communication between the CNS and the periphery (1,2). Among these, intra-cortical microelectrodes have been suggested to be particularly useful for restoration of voluntary motor control in severely paralyzed patients (1). While less invasive methods to partially restore motor function are available, only microelectrodes have the ability to record from populations of single neurons, and thus have the potential to decode neuronal activity related to fine motor control. Unfortunately, despite the great promise for future therapeutic treatments, the

Km57@drexel.edu.

implementation of intra-cortical single neuron recordings has been limited by the loss of neural recordings over time after implantation (3,4).

Early hypotheses concerning the reason for such failure focused on the development of a glial scar (5,6); however, more recent studies have suggested that failure is due, at least in part, to loss of neurons within the recording zone immediately adjacent to the microelectrode (<200μm) (7). While neuronal cell death and loss of neurites continues for at least 16 weeks post-implantation (8), the majority of the loss occurs within the first two weeks (8,9). During insertion, microelectrodes mechanically damage the membranes of neurons and glial cells alike. Intracellular proteins are released into the extracellular environment and trigger an acute inflammatory response around the microelectrode. Microglia, oligodendrocyte precursors and astrocytes release signaling proteins into the local environment initiating a cascade of events that leads to glial cell proliferation (10), and this inflammation is accompanied by neurodegeneration (8,10). To mitigate this biological response, researchers have either focused on biomaterials efforts (changing the size, shape, or material properties of the implant (5,11,12) or the use of pharmacologic anti-inflammatory agents. (3,13–15). To date, however, no studies have examined strategies that directly repair the initial damage due to the microelectrode insertion in-vivo. Recent in-vitro work has shown that the triblock copolymer Poloxamer (P-188) promotes cell viability and cell recovery by sealing ruptured cell membranes in mechanically injured neurons (16,17) thereby preventing post-injury axonal bead formation (11,18) and enhancing overall neuroprotection. To test whether Poloxamer can mitigate in-vivo cellular damage and inflammation from electrode insertion, this study quantifies glial activation and changes in neuronal cell density due to the chronic implantation of electrodes coated with Poloxamer and uncoated controls at two, four and six weeks post implantation in adult male Long-Evans rats. Unlike other chronic implant biocompatibility studies, we have affixed the implants to the skull for the purposes of making periodic extracellular recordings to verify electrode function.

2. Methods and Materials

2.1 Microelectrodes

As part of ongoing work, microelectrodes were manufactured from porous silicon substrates with ceramic insulation. The porous substrate was chosen both to ease the initial loading of Poloxamer onto the surface and because of previous findings that indicate a reduction in glial activation in porous over smooth electrodes (18). These ceramic based multi-site electrode arrays (CBMSE) were fabricated according to methods previously described by Moxon et al. (11). The width of the electrode at the tip was 66.4μm and tapered to 113μm at the most proximal recording site (Figure 1D). Electrode fabrication was performed in clean room facilities and additional handling was kept to a minimum to reduce contamination. As a result, no special measures were taken to sterilize electrodes against endotoxin. All electrodes were sterilized prior to implantation by sonication for 5 minutes in DI water followed by 5 minutes in 70% isopropyl alcohol.

2.2 Implantation of Microelectrodes

All animal procedures were performed utilizing sterile techniques approved by the Drexel University Institutional Animal Care and Use Committee (IACUC) and adhered to National Institute of Health (NIH) guidelines. Adult male Long-Evans rats between 275-299g were used in this study. Animals were intubated and anesthetized using 4.5 % isoflourane in oxygen at 2 L / min. The rat's head was shaved and the area of interest was disinfected with isopropyl alcohol followed by a Betadine swab. Ophthalmic ointment (Altaire Pharmaceuticals, Aquebogue NY) was applied to animal's eyes to prevent corneal damage. Each animal was placed on a stereotactic frame (Cartesian Research Inc, Portland OR), and anesthesia was maintained in oxygen in 0.5 L/min for the duration of the surgery. A midline incision was made in the skin, and the skull was centered to bregma on the stereotactic frame. A 3mm × 5mm craniotomy was drilled for each of two electrodes at 2.5 mm bilaterally and 0 mm anterior to bregma. In order to support the electrode cap, a series of smaller anchoring points were drilled in the skull for placement of four metal screws. The bone plug of the craniotomy was carefully removed and the dura was gently pierced with fine micro-forceps. Immediately prior to insertion, one of two electrodes was loaded with Poloxamer by two 5 minute immersions in 100μm Poloxamer (Sigma) dissolved in saline separated by 10 minutes of air drying. The remaining control electrode was dipped in sterile saline with the same procedure. After a final 10 minutes of air drying, the microelectrodes were inserted into the cortex at a rate of 50μm/min until the most ventral recording site reached the deep layers of the cortex and at least one neuron was observed on all four sites (approximately 1.8 mm). During the electrode insertion, saline was applied to the open craniotomies to reduce brain exposure and to minimize iatrogenic damage. During insertion, neural activity was monitored using a high speed data acquisition system using a unity gain headstage connected to an external preamplifier (Plexon, Dallas TX) in a manner similar to our previously published work (18), to ensure that Poloxamer was not interfering with electrode recording ability. After insertion, the craniotomies were covered with dental acrylic, paying particular attention to leaving the electrode interface connectors exposed. The skin incision was then closed with surgical staples and the animal was allowed to recover from anesthesia on a heating pad at 25° C until it regained normal gait and grooming behavior.

Neuronal activity was recorded during electrode implantation and at weeks 1, 2, 4 and 6 post implantation. For each recording session, single neurons were discriminated from broadband recordings as described in previous publications (11). In brief, animals were anesthetized and a tethered headstage amplifier (100x) was connected to the exposed Omnetics connector that affixes the electrode to the animals skull. Signals were further amplified by a 1000x preamplifier and sampled at 40 kHz. Broadband signals were bandpass filtered form 600Hz – 10kHz, displayed on a computer screen and played over audio speakers. Neuronal activity was examined as the cutaneous surface of the skin and body hairs were stimulated with a wooden probe. A threshold above the mean and equal to 5 times the variance of the signal was set and a recording site with at least one discriminable single unit that exceeded the threshold was identified as active.

2.3 Tissue Processing for Immunohistochemistry

To measure the effects of neural repair using Poloxamer, animals were euthanized at two weeks (n = 5), four weeks (n = 5), and six weeks (n = 5) post implantation. The animals were sacrificed with an overdose of Euthasol (Virbac, Fort Worth, TX) and then perfused transcardially with 0.5 L of ice cold PBS (Sigma) followed by 0.5 L of ice cold 4% paraformaldehyde (Fisher). Brains were removed such that the implanted neural probes remained intact. After fixation of the brain in paraformaldehyde for 48 hours, the brains were dissected and the electrodes were retrieved from the tissue. The brains were placed into 30% sucrose in PBS solution (4° C) to equilibrate for three to five days. After the equilibration period, the tissue was frozen and sections of 20 μm thickness were cut using a Leica CM3500 cryotome in the horizontal plane through the depth of the cortex (1 mm). The sections were collected using a low-distortion tape system, serially sorted into four sets and mounted onto slides (19). There were approximately 20 slices per brain per set.

2.4 Immunohistochemistry

Sections from cortex were stained to measure the size of the hole left by the microelectrode and to observe brain tissue response. After mounting onto slides, cortical sections were washed in PBS and blocked in goat serum for an hour at room temperature. Sections were then incubated overnight with one of 3 primary antibodies or nissl myelin stained. Group one received mouse monoclonal Anti-CD68 (ED1, Serotek, 1:1000) to stain for reactive macrophages and microglia. The second group received mouse monoclonal anti-Neuronal Nuclei (NeuN, Millipore, 1:1000) to stain for neuron cell nuclei. Group three received rabbit polyclonal anti-glial fibrillary acidic protein (GFAP, Sigma, 1:1000) to identify astrocytes, and group four was stained with nissl myelin staining. After the incubation in primary antibodies, sections were washed in PBS and incubated in appropriate secondary antibodies labeled with a fluorescent marker (Jackson Immuno Research) for two hours at a 1:100 dilution. All fluorescently stained sections received a DAPI counter stain (Thermo Scientific).

2.5 Hole Size Analysis

The functional recording radius for microelectrodes is approximately 140μm from the recording site (20). For our electrodes, these sites are located at the surface of a silicon shank or ~30-60μm from the center of the electrode. Thus we expect that neurons found in the 0-100μm and the 100-200μm bins will be within the functional range for extracellular recordings. During explantation, some degree of tissue loss within these regions was unavoidable (5,7). To ensure that cell counts were not being biased by such loss of tissue, the explant hole size was characterized for each sample. Fluorescent images were taken at 2.5× magnification around the implant site and then converted into grayscale. Hole areas were determined from these images (ImageJ, NIH).

2.6 Qualitative Analysis Stereological Techniques for Cell Counts

Design-based stereology was used to characterize the cellular presence in the histological sections because it allows for three-dimensional interpretation of structures from each section and is an assumption free method that can be used to study objects of different

shapes (21). A further advantage of this method is that it estimates the total number of objects in any three dimensional volume regardless of that volume's shape or size. Cell counts were made directly from the tissue slices, rather than static images processed by a camera, allowing for the verification of cell presence through multiple focal planes. For the photomicrographs in Figures 5, 6 and 8, the contrast and brightness were adjusted to highlight cell presence and explant site, but such post-processing steps were not utilized during data collection. Cell counts were performed using a Firefly Microfire camera (Olympus America, Inc) attached to a Zeiss Axioplan, which in turn was connected to a Dell workstation using Steroinvestigator Software (Microbrightfield, Inc, Williston, VT). A motorized stage was controlled by the software suite to allow for precise tracking along the X and Y and Z axes. Sectioned tissue samples were cursorily observed at a magnification of 2.5X. The center of each electrode hole was located and served as a reference for the coordinate system used for subsequent analysis. Using a contour tool the electrode hole was traced and a circle of 500μm radius was automatically generated about the center of the delineated hole. A standard optical fractionator probe was then used for quantitative analysis of each fluorescent antibody for astrocytes (GFAP), neurons (NeuN), and microglia (ED1) at a higher magnification of 100X oil objective. To do so, a sampling grid was generated within the traced contour and an unbiased counting probe was placed within each grid box (Figure 1A). The sampling grid and counting frame dimension were chosen to create a 17.3% sampling percentage within the selected contour. At each sampling site, the tissue was scanned in the Z axis, and cell presence was acknowledged when a nucleus came into focus. The counting frame area was selected to be 2500μm^2 (in X, 50μm; in Y, 50μm) and the grid size of 120μm × 120μm. The thickness of interest (optical dissector height) was set at 12μm leaving a 4μm top and bottom guard zone. To avoid estimation errors, cells were not counted within the guard zone areas. Cell counts were then normalized as described in the following section.

2.7 Cell Density Profile Across Distance

During cell counting, the coordinates of each cell were recorded with respect to the center of the electrode hole (origin) and the radial distance from the origin to the cell was determined in microns. The cells were binned in 5 annular domains based on distance from the origin: < 100 μm, 100-200μm, 200-300μm, 300-400μm, and 400-500μm. Because the width of the recording electrode varied from 66μm to 115μm, the inner most domain (<100μm) was mostly occupied by the electrode itself. For each slice and each cell type, the total number of cells within each annular domain ware reported as densities by dividing the cell counts by the volume sampled. Because we were interested in changes in cell density around the microelectrode, cell densities for each annular domain were normalized to a baseline cell density defined in the 400-500μm annular domain of the control electrode (i.e. the cell density of control in the 400-500μm annular domain equals 100%). For the <100μm domain, the amount of tissue remaining after explant was variable both due to the shape of the microelectrode and the fact that some tissue remained on the electrode as has been observed in similar studies (5,7). Therefore, approximately two-thirds of the counting frames were not completely filled with tissue and those frames were discarded. The remaining frames were analyzed separately.

2.8 Intensity Analysis

In addition to determining cellular densities, protein expression is of particular interest as a marker of cellular activation. To be consistent with earlier work (7), an intensity based method was used to assess the extent to which GFAP expression differed in the tissue surrounding Poloxamer coated and control microelectrodes. Using the same microscope setup, 10X fluorescent images were acquired, for the GFAP marker, around the implant site. Image analysis was then performed using a custom program developed in MATLAB in a manner similar to He et al., 2006 (22). To account for variations in staining intensity between subjects, the intensity of staining in tissue more than 1 mm from injury site was subtracted from the intensity around the electrode hole. Then, for each slice, a set of ten equidistant lines that spanned the full diameter of the electrode hole was superimposed on the image. The orientation of the lines with respect to the hole was random. Using a consistent intensity scale, the intensity of staining was quantified across the ten lines to create an intensity profile. For each line, the edge of the hole was identified visually. The average magnitude of the intensity was reported in four intervals from the tissue edge: 0-50μm, 50-100μm, 100-150μm and 150-200μm.

2.9 Statistical Analysis

To assess whether Poloxamer interfered with the ability to record single units, the number of active recording sites (maximum = 4) at weeks 1, 2, 4 and 6 on coated microelectrodes was compared to those on noncoated microelectrodes using paired t-tests, separately for each time point. Differences were considered significant at $p < 0.05$.

To verify that no bias was introduced due to tissue loss across treatments and implantation duration, differences in the hole size around the microelectrodes were compared using a two-way analysis of variance (ANOVA) with fixed factors of duration and treatment with $p < 0.05$ considered significant.

To assess difference in immunoreactivity in the annular domain closest to the microelectrode (< 100μm) normalized density of ED1, GFAP and NeuN positive cells around Poloxamer treated microelectrodes were separately compared to the density of cells around control electrodes using paired t-tests. Due to the fact that this domain was largely filled by the microelectrode, the number of usable sampling frames was limited and so this annular domain was tested separately from the other domains. (see section 2.6). A Bonferroni corrected significance threshold of $p < 0.016$ was used to determine significance.

To assess difference in immunoreactivity at greater distances from the microelectrode (100μm-500μm), normalized density of ED1, GFAP and NeuN positive cells around Poloxamer treated microelectrodes were separately compared to densities of cells around control electrodes using a repeated measures ANOVA with three within subject factors (distance, treatment, depth) and one between subject factor (duration) using $p < 0.05$ for significance. Finally planned comparisons using Student's t-test with Bonferroni correction ($p < 0.004$) were used to identify differences between experimental groups at specific time points when warranted.

3. Results

3.1 Characterization of Tissue Loss and Immunoreactivity adjacent to microelectrrode

To determine if Poloxamer interfered with our ability to record single neurons, the number of active recording sites on Poloxamer coated microelectrodes was compared to those on control electrodes. During implantation, more than 90% of the recording sites for both Poloxamer coated and control microelectrodes had at least one discriminable sites remained stable at approximately 50% throughout differences between the number of active recordin microelectrodes electrodes ($p > 0.05$; paired t-test), indicating that Poloxamer did not compromise the ability to detect single neuron activity.

Because the effects of implantation are likely to be greatest near the electrode surface, variations in the amount of tissue removed during explanation (5,7) would affect the variability of the measurements and potentially bias the observations. No significant differences were found in hole size across treatments ($F(1) = 0.418$, $p > 0.5$), duration ($F(2) = 0.74$, $p > 0.5$) or the duration treatment interaction ($F(2)=0.558$, $p > 0.5$) Thus, any tissue that was removed during explants of the microelect trode was similar across groups.

Finally, to assess the impact of Poloxamer in the remaining tissue closest to the microelectrode, the cell density within 100 μm of the electrode were compared between groups (Figure 3). Control electrodes showed significantly more ED1 and GFAP immunoreactivity around the microelectrodes compared to Poloxamer coated microelectrodes ($t(84) = -3.54$ $p < 0.016$, $t(83) = -2.68$, $p < 0.016$). Moreover, there were fewer NeuN positive cells identified around control electrodes compared to the Poloxamer coated microelectrodes ($t(75) = 2.526$, $p < 0.016$). These data suggest that Poloxamer reduces the inflammatory response around the microelectrode, increasing the density of neurons immediately adjacent to the microelectrode.

3.2 Peri-electrode Cellular Response

3.2.1 Microglial Response (EDI)—Across 15 animals, 5174 ED1+ cells were counted. For EDI immunoreactivity, the omnibus test showed significant main effects for distance ($F(1.043,12.515) = 22.428$, $p < 0.0001$) and treatment ($F(1,12) = 71.534$, $p < 0.0001$) but not duration or depth. The main effect of treatment demonstrated a significant decrease in microglial cell density in Poloxamer coated electrodes over control (Figure 4, top left). Because the main effect of duration failed to provide insight into the time course of action of Poloxamer in vivo, planned comparisons with Bonferroni correction were made between coated and control electrodes at 2, 4 and 6 week durations. ED1 immunoreactivity for the coated group was significantly less than for the control group at two weeks ($t(131.865) = 3.926$, $p < 0.001$) and four weeks ($t(133.736) = 3.099$, $p < 0.01$) but not at six weeks post implantation (Figure 4, top right).

In a similar manner, the effect of distance was examined independently for each time point post-implant (Figure 5). At two and four weeks, Poloxamer coated microelectrodes had fewer ED1 positive cells compared to control at a majority of distances tested. And, in agreement with planned comparisons reported above, there were no difference at 6 weeks.

3.2.2 Astrocyte Cell Density—Astrocyte cell presence was characterized by GFAP staining of slides from 15 animals containing a total of 4873 GFAP+ cells. Similar to the ED1 staining condition, the omnibus test showed significant main effects for both treatment and distance but not for duration or depth. ($F(1,12) = 15.997$, $p < 0.005$) In addition, there were no significant interactions between any of the main effects. Electrodes coated with Poloxamer recruited fewer astrocytes than control electrodes (Figure 4, middle left). To evaluate the effects of Poloxamer treatment on the astrocytic response over time, planned comparisons were made between Poloxamer and control electrodes at two, four, and six week implant durations (Figure 4, middle right). At two weeks, astrocyte cell density surrounding Poloxamer treated microelectrodes was significantly lower than that around controls ($t(196.768) = 4.467$, $p < 0.0001$), but not at four or six weeks, further supporting robust effects of Poloxamer at shorter time periods. This difference at two weeks was mainly due to an elevated number of GFAP positive cells around control electrodes with little difference in the number of GFAP positive cells within the 500 micron annulus for Poloxamer treated microelectrodes (Figure 6).

3.2.3 Astrocyte Protein Expression—To provide a view that is consistent with earlier work (7), line intensity profiles were taken as a function of distance away from the edge of scar in GFAP stained samples. ANOVA showed significant main effects for treatment ($F(1,380) = 13.443$, $p < 0.001$), distance ($F(1,380) = 17.843$, $p < 0.001$) and duration ($F(1,380) = 119.858$, $p < 0.001$). As was the case for the GFAP cell counts, there was a significant decrease in the measured fluorescent intensity of GFAP stained tissue surrounding coated electrodes as compared to untreated controls. Planned comparisons revealed that at 2 weeks after implantation, GFAP intensity was significantly decreased compared to control ($t(15) = 3.0304$, $p < 0.01$) Consistent with cell density analysis, above, at 4 and 6 weeks, there were no differences in intensity of GFAP staining (Figure 7).

3.2.4 Neuronal Survival (NeuN)—Neuronal presence around the implanted electrode was characterized by using the NeuN stain for neuronal nuclei. Across 15 animals 10,499 neurons were observed. We found a significantly greater density of neurons around Poloxamer coated electrodes, as indicated by the significant omnibus for treatment (Figure 4 bottom left, $F(1,12) = 11.018$, $p < 0.01$). The omnibus also showed a significant main effect of distance ($F(1.676,20.115) = 10.150$, $p < 0.005$) but not for duration or depth, as was observed in the ED1 and GFAP staining condition. To assess the effect of implant duration on the response to treatment, planned comparisons (with Bonferroni correction) of peri-implant neuron density were made between control and Poloxamer coated electrodes at two, four and six weeks post implant (Figure 4, bottom right). These comparisons show that neuron density was higher surrounding Poloxamer electrodes at two weeks ($t(196.768) = 3.81$, $p < 0.0005$), but not at four or six weeks post implant. When examining the effect of distance, in a manner complimentary to the ED1 and GFAP staining, the loss of neurons was greatest closest to the microelectrode, within the 200μm relevant for neural recording (Figure 8).

4. Discussion

The results of this study suggest that a surface coating of Poloxamer can reduce the acute inflammatory response to surgical implantation of microelectrodes into the CNS. Markers of significant neuroprotective effects (increased neuron survival or reduced gliosis) were present at 2 weeks post implantation (ED1, GFAP, & NeuN) and at 4 weeks (ED1). By 6 weeks, however, there was no significant difference between the Poloxamer coated electrodes and uncoated electrodes in all metrics. These results suggest that further testing with Poloxamer to reduce cell death and gliosis around the microelectrode is warranted, especially if controlled, long-term release can be achieved.

4.1 Assessing Neuroprotection

Three staining conditions were used to assess the inflammatory response to chronic implantation. The rationale for choosing these stains is provided in brief. Surgical insertion of a microelectrode tears dendritic and axonal processes and will induce some degree of neuronal cell death (4,18) Beyond this initial mechanical trauma, neuron loss about implanted electrodes (characterized by NeuN stain) may be attributed to the release of cytotoxic mediators to the local environment, displacement from growing scar tissue, and damage caused by persistent micromotion (23). Concomitant vascular damage and the release of inflammatory mediators and chemotactic factors from dying cells, attract and activate circulating monocytes/nearby microglia (24) and have been shown to significantly affect the degree of glial scaring and cell death around neuroprostheses (15).The number of phagocytic cells and their state of activation, as characterized by ED1 staining, can therefore provide a gauge for assessing immune response (4,25,26).

In tandem, the recruitment of glial cells contributes to the formation of an astrocyte barrier separating the injury site from healthy tissue (4,5). Astrocyte participation in glial scar formation includes changes in metabolic state and secretion of neural growth factor, which helps in repairing damaged neural tissue (27). Reactive astrocytes exhibit phenotypic changes characterized by hypertrophy and increase in expression of glial fibrillary acidic protein (GFAP), which is critical to astrocyte function and their ability to support neighboring damaged neurons (10) and as such their presence and activity (characterized by GFAP staining) reflects the amount of injury sustained.

Long term success of implanted extracellular electrodes depends on electrodes maintaining their proximity to active neurons so that extracellular potentials may be recorded. There are two modes by which the electrode may fail to remain in proximity to the neuronal population of interest. First, the aforementioned glial response may form a physical barrier. A majority of neurons will fire with an amplitude that can be detected within a radius of 140μm of an implanted electrode (20), so a scar of sufficient size may attenuate the extracellular voltage changes beyond our ability to detect. Second, the local neuronal population may die off, due, in part, to mechanical trauma during implantation or subsequent micro-motion (23). In either case, a neuron-specific marker such as NeuN will demonstrate the extent to which the local population is removed from the implanted electrode.

4.2 Time Course of Cellular Response

For the six weeks studied here, the tissue closest to the electrode (<100μm from hole center) maintained significantly more neurons and fewer activated glia (ED1 and GFAP positive cells). Beyond this innermost domain, significant effects could still be observed in a time dependent manner with all effects lost by 6 weeks post implantation. Given Poloxamer's theorized mechanism of action, one would expect that the most pronounced differences between Poloxamer coated and control implants would be present immediately after implantation. In fact, we found a significant reduction in neuronal cell loss and reduced upregulation of cells associated with the inflammatory response normally associated with microelectrode insertion. Of course Poloxamer is not completely effective and in the 200μm adjacent to the electrode surface there is a reduction in the density neurons compared to baseline. This is in accord with other similarly coated single shank electrode implant studies that show a steep loss of neurons in the early immune response up to 150μm from the implant surface (7,14,15,28) with neuron loss extending further up to 300μm from the implant surface in the late immune response (28). It is possible that higher loading doses, controlled, long-term release or parallel adjuvant therapy may take advantage of this recovery and delay the onset of chronic neuron loss or avoid it all together. The glial response shows a similar finding at 2 weeks, with significantly lower peri-electrode astrocyte and glial cell density. Astrocytes were observed to have long thin easily resolved cellular processes indicating newly migrated cells that have not yet undergone activation. Cell counts were fairly uniform within the 400μm of the implant surface with a slight trend towards decreasing in count at greater distances from the implant surface. Though not statistically significant at every distance, the counts were consistently lower in Poloxamer coated implants than in controls. Similarly ED1+ cell counts were also significantly depressed around Poloxamer coated electrodes. Therefore, the impact of Poloxamer in the early stages of glial scar formation was substantial.

By 4 weeks post implantation, the number of ED1 positive cells remains attenuated compared to control but any effect of Poloxamer on the number of neurons or the density of GFAP positive cells was lost in the annular domains beyond 100 microns from the hole center. Although significant differences between Poloxamer and control electrodes were lost, there was a trend toward fewer GFAP positive cells and more neurons around the Poloxamer treated microelectrodes. On possibilities is that by reducing the extent of the initial cellular damage, fewer pro-inflammatory cytokines and immunogenic intracellular moieties are available to recruit microglia and their response was correspondingly attenuated. This observed activation of astrocytes and the formation of an astrocytic sheath are in agreement with other studies of chronic implant response (4,5,8,13).

In the late immune response (6 weeks post implantation), the effects of Poloxamer appear to be lost as no differences between control and Poloxamer coated implants could be noted in any of the staining conditions. This may be due to several factors including the depletion of Poloxamer over time and a fundamental change in the type of damage that occurs as the immune response progresses. The compliance mismatch between the electrode and surrounding tissue and micro-motion inherent to tethered implants could cause persistent mechanical trauma and cellular necrosis (23) that could potentially be mitigated by

Poloxamer if delivered chronically. However, prolonged microglial activation and the corresponding release of reactive oxide species (7) could also progressively damage and destroy remaining neurons (via an apoptotic rather than necrotic mechanism). While there is evidence to suggest that Poloxamer does prevent apoptotic cell death in-vitro in response to mechanical trauma (17), it is unknown whether its function is similar in-vivo under chronic inflammatory conditions, and further work is needed to better characterize the long term immune response to Poloxamer coated implants.

4.3 Summary

The purpose of this study was to explore the use of Poloxamer P-188 as a neurorepair agent during chronic extracellular recordings in-vivo. The biologic failure mode for chronic neural implants is associated with the development of a glial scar including the recruitment of astrocytes and microglia to the implant-tissue interface. (4) Concomitantly there is a diminishing of the local neuron population, either from cell death or displacement by the growing glial scar (7). Thus, to ensure the ability to make chronic extracellular recordings of single neurons from such implants, it is necessary to mitigate the degree of glial scar formation and associated neuronal loss. Many groups have attempted to address this problem with the use of anti-inflammatory agents (delivered either locally or systemically) or through non-immunogenic electrode coatings that discourage the foreign body response (12,14,15,29). However, these methods are limited in that they attempt to modulate the body's responses and not the underlying cause, namely mechanical trauma from a foreign body and subsequent necrotic cell death. Poloxamer has been demonstrated in numerous studies to repair/prevent further damage caused to cellular membranes in diverse cell types including: erythrocytes (ex-vivo), myocytes (in-vitro and in-vivo) neurons (in-vitro) (16,30,31). The present study has demonstrated that, Poloxamer also has a role to play in the in-vivo repair of implantation associated damage to neurons and glia. While the apparent neuroprotective effects of Poloxamer appear to be limited to the acute immune response, further optimization and combination therapies may prolong Poloxamer's neuroprotective effects. This use of Poloxamer potentially targets an as yet unexplored option for attenuating the immune response to chronic micro-electrode implantation.

In summary, this study demonstrates that a simple dip coating of Poloxamer P-188 significantly increases peri-electrode neuronal survival and decreases immune response in the one month following implantation, but the apparent neuroprotective effects are lost by 6 weeks. The reason for this loss of efficacy may be due to simple depletion, or due to a shift in the mechanism by which cells are damaged in the chronic immune response. Regardless of failure mode, Poloxamer may prove to be a useful tool for short term implantation and acute projects where recording quality must be optimized but long term survival is of lesser importance. It may also change the way in which Poloxamer and similar surfactants are used in current drug delivery paradigms.

Acknowledgments

This work was supported by grant 5R21MH081248-02 from the National Institute of Health and by a grant from the Coulter Foundation.

References

1. Hochberg LR, Donoghue JP. Sensors for brain-computer interfaces. IEEE Engineering in Medicine and Biology Magazine [Internet]. Sep; 2006 25(5):32–8. Available from: http://ieeexplore.ieee.org/lpdocs/epic03/wrapper.htm?arnumber=1705745.
2. Sanchez JC, Carmena JM, Lebedev M, Nicolelis M a L, Harris JG, Principe JC. Ascertaining the importance of neurons to develop better brain-machine interfaces. IEEE transactions on bio-medical engineering [Internet]. Jun; 2004 51(6):943–53. Available from: http://www.ncbi.nlm.nih.gov/pubmed/15188862.
3. Grill WM, Norman SE, Bellamkonda RV. Implanted neural interfaces: biochallenges and engineered solutions. Annual review of biomedical engineering [Internet]. Jan.2009 11:1–24. Available from: http://www.ncbi.nlm.nih.gov/pubmed/19400710.
4. Polikov VS, Tresco P a, Reichert WM. Response of brain tissue to chronically implanted neural electrodes. Journal of neuroscience methods [Internet]. Oct 15; 2005 148(1):1–18. Available from: http://www.ncbi.nlm.nih.gov/pubmed/16198003.
5. Szarowski DH, Andersen MD, Retterer S, Spence AJ, Isaacson M, Craighead HG, et al. Brain responses to micro-machined silicon devices. Brain Research [Internet]. Sep; 2003 983(1-2):23–35. Available from: http://linkinghub.elsevier.com/retrieve/pii/S0006899303030233.
6. Vetter RJ, Williams JC, Hetke JF, Nunamaker E a, Kipke DR. Chronic neural recording using silicon-substrate microelectrode arrays implanted in cerebral cortex. IEEE transactions on bio-medical engineering [Internet]. Jun; 2004 51(6):896–904. Available from: http://www.ncbi.nlm.nih.gov/pubmed/15188856.
7. Biran R, Martin DC, Tresco P a. Neuronal cell loss accompanies the brain tissue response to chronically implanted silicon microelectrode arrays. Experimental neurology [Internet]. Sep; 2005 195(1):115–26. Available from: http://www.ncbi.nlm.nih.gov/pubmed/16045910.
8. McConnell GC, Rees HD, Levey AI, Gutekunst C-A, Gross RE, Bellamkonda RV. Implanted neural electrodes cause chronic, local inflammation that is correlated with local neurodegeneration. Journal of neural engineering [Internet]. Oct.2009 6(5):056003. Available from: http://www.ncbi.nlm.nih.gov/pubmed/19700815.
9. Winslow, BD.; Christensen, MB.; Yang, W-K.; Solzbacher, F.; Tresco, P a. Biomaterials [Internet]. Vol. 31. Elsevier Ltd; Dec. 2010 A comparison of the tissue response to chronically implanted Parylene-C-coated and uncoated planar silicon microelectrode arrays in rat cortex; p. 9163-72.Available from: http://www.ncbi.nlm.nih.gov/pubmed/20561678 [cited 2011 Jul 18]
10. Zhong Y, Bellamkonda RV. Biomaterials for the central nervous system. Journal of the Royal Society, Interface / the Royal Society [Internet]. Sep 6; 2008 5(26):957–75. Available from: http://www.pubmedcentral.nih.gov/articlerender.fcgi?artid=2475552&tool=pmcentrez&rendertype=abstract.
11. Moxon K, Leiser SC, Gerhardt G a, Barbee K, Chapin JK. Ceramic-based multisite electrode arrays for chronic single-neuron recording. IEEE transactions on bio-medical engineering [Internet]. Apr; 2004 51(4):647–56. Available from: http://www.ncbi.nlm.nih.gov/pubmed/15072219.
12. He, L.; Lin, D.; Wang, Y.; Xiao, Y.; Che, J. B, Biointerfaces [Internet]. Vol. 87. Elsevier B.V.; Oct 15. 2011 Electroactive SWNT/PEGDA hybrid hydrogel coating for bio-electrode interface. Colloids and surfaces; p. 273-9.Available from: http://www.ncbi.nlm.nih.gov/pubmed/21676598 [cited 2011 Jul 19]
13. Spataro L, Dilgen J, Retterer S, Spence a. J, Isaacson M, Turner JN, et al. Dexamethasone treatment reduces astroglia responses to inserted neuroprosthetic devices in rat neocortex. Experimental neurology [Internet]. Aug; 2005 194(2):289–300. Available from: http://www.ncbi.nlm.nih.gov/pubmed/16022859.
14. Zhong Y, Bellamkonda RV. Dexamethasone-coated neural probes elicit attenuated inflammatory response and neuronal loss compared to uncoated neural probes. Brain research [Internet]. May 7.2007 1148:15–27. Available from:http://www.pubmedcentral.nih.gov/articlerender.fcgi?artid=1950487&tool=pmcentrez&re ndertype=abstract.

15. Grand L, Wittner L, Herwik S, Göthelid E, Ruther P, Oscarsson S, et al. Short and long term biocompatibility of NeuroProbes silicon probes. Journal of neuroscience methods [Internet]. Jun 15; 2010 189(2):216–29. Available from: http://www.ncbi.nlm.nih.gov/pubmed/20399227.

16. Serbest G, Horwitz J, Barbee K. The effect of poloxamer-188 on neuronal cell recovery from mechanical injury. Journal of neurotrauma [Internet]. Jan; 2005 22(1):119–32. Available from: http://www.ncbi.nlm.nih.gov/pubmed/15665607.

17. Serbest G, Horwitz J, Jost M, Barbee K. Mechanisms of cell death and neuroprotection by poloxamer 188 after mechanical trauma. The FASEB journal□: official publication of the Federation of American Societies for Experimental Biology [Internet]. Feb; 2006 20(2):308–10. Available from: http://www.ncbi.nlm.nih.gov/pubmed/16371428.

18. Moxon K, Hallman S, Aslani A, Kalkhoran N, Lelkes P. Bioactive properties of nanostructured porous silicon for enhancing electrode to neuron interfaces. Journal of Biomaterials Science, Polymer Edition [Internet]. VSP, an imprint of Brill. 2007; 18(10):1263–81. Available from: http://www.ingentaconnect.com/content/vsp/bsp/2007/00000018/00000010/art00003.

19. Nissanov J, Bertrand L, Tretiak O. Cryosectioning distortion reduction using tape support. Microscopy research and technique [Internet]. May 1; 2001 53(3):239–40. Available from: http://www.ncbi.nlm.nih.gov/pubmed/11301500.

20. Buzsáki G. Large-scale recording of neuronal ensembles. Nature neuroscience [Internet]. May; 2004 7(5):446–51. Available from: http://www.ncbi.nlm.nih.gov/pubmed/15114356.

21. West, MJ. Design-based stereological methods for counting neurons. In: Thomas Sutula, AP., editor. Do seizures damage the brain [Internet]. Elsevier; 2002. p. 43-51.Available from: http://www.sciencedirect.com/science/article/pii/S0079612302350064

22. He W, McConnell GC, Bellamkonda RV. Nanoscale laminin coating modulates cortical scarring response around implanted silicon microelectrode arrays. Journal of neural engineering [Internet]. Dec; 2006 3(4):316–26. Available from: http://www.ncbi.nlm.nih.gov/pubmed/17124336.

23. Kim Y-T, Hitchcock RW, Bridge MJ, Tresco P a. Chronic response of adult rat brain tissue to implants anchored to the skull. Biomaterials [Internet]. May; 2004 25(12):2229–37. Available from: http://linkinghub.elsevier.com/retrieve/pii/S0142961203007440.

24. Bjornsson CS, Oh SJ, Al-Kofahi Y a, Lim YJ, Smith KL, Turner JN, et al. Effects of insertion conditions on tissue strain and vascular damage during neuroprosthetic device insertion. Journal of neural engineering [Internet]. Sep; 2006 3(3):196–207. Available from: http://www.ncbi.nlm.nih.gov/pubmed/16921203.

25. Fawcett JW, Asher R a. The glial scar and central nervous system repair. Brain research bulletin [Internet]. Aug; 1999 49(6):377–91. Available from: http://www.ncbi.nlm.nih.gov/pubmed/10483914.

26. Kreutzberg GW. Microglia: a sensor for pathological events in the CNS. Trends in neurosciences [Internet]. Aug; 1996 19(8):312–8. Available from: http://www.ncbi.nlm.nih.gov/pubmed/8843599.

27. Goss JR, O'Malley ME, Zou L, Styren SD, Kochanek PM, DeKosky ST. Astrocytes are the major source of nerve growth factor upregulation following traumatic brain injury in the rat. Experimental neurology [Internet]. Feb; 1998 149(2):301–9. Available from: http://www.ncbi.nlm.nih.gov/pubmed/9500953.

28. Azemi, E.; Lagenaur, CF.; Cui, XT. Biomaterials [Internet]. Vol. 32. Elsevier Ltd; Jan. 2011 The surface immobilization of the neural adhesion molecule L1 on neural probes and its effect on neuronal density and gliosis at the probe/tissue interface; p. 681-92.Available from: http://www.ncbi.nlm.nih.gov/pubmed/20933270 [cited 2011 Jul 26]

29. Zhou Q, Li T, Li C, Ye M, Lu Y, Duan Y. Biocompatibility of implantable electrodes coated with PVA films in the brain of rats: a histological evaluation. Journal of Wuhan University of Technology-Mater. Sci. Ed. [Internet]. Jul 9; 2009 24(3):393–6. Available from: http://www.springerlink.com/index/10.1007/s11595- 009-3393-5.

30. HANNIG J. Poloxamine 1107 sealing of radiopermeabilized erythrocyte membranes. International Journal of Radiation Biology [Internet]. 1999; 75(3):379–85. Available from: http://informahealthcare.com/doi/abs/10.1080/095530099140555.

31. Murphy AD, McCormack MC, Bichara D a, Nguyen JT, Randolph M a, Watkins MT, et al. Poloxamer 188 protects against ischemia-reperfusion injury in a murine hind-limb model. Plastic and reconstructive surgery [Internet]. Jun; 2010 125(6):1651–60. Available from: http://www.ncbi.nlm.nih.gov/pubmed/20517088.

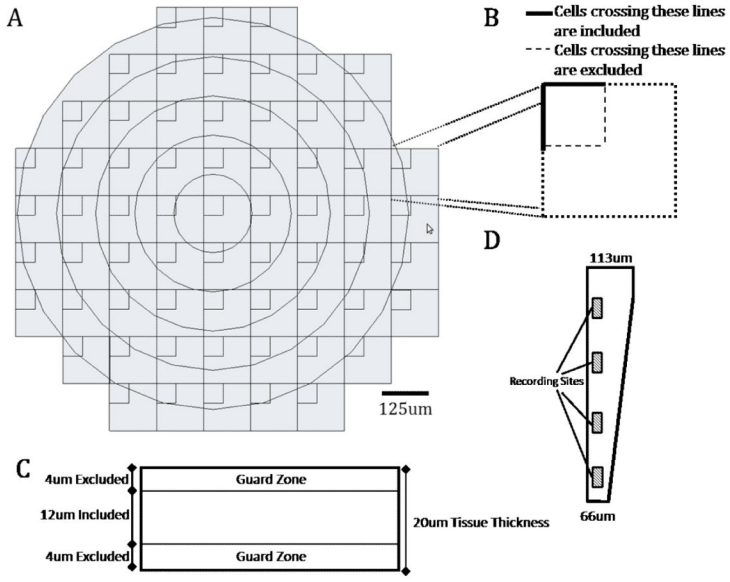

Figure 1.

A) Schematic representation of the array of counting frames that was superimposed onto tissue slices using the Stereoinvestigator software package. B) Blowup of a single counting frame. Cells crossing the solid boundary lines were included in the count while cells crossing the dashed boundary lines were not, thereby serving to prevent double counting cells. C) A schematic cross section of the tissue slice illustrating the 4um guard zones that were not sampled to reduce influence from non uniform tissue slices. D) Schematic of the tip of the CBMSE electrode shaft that was implanted in rat cortex.

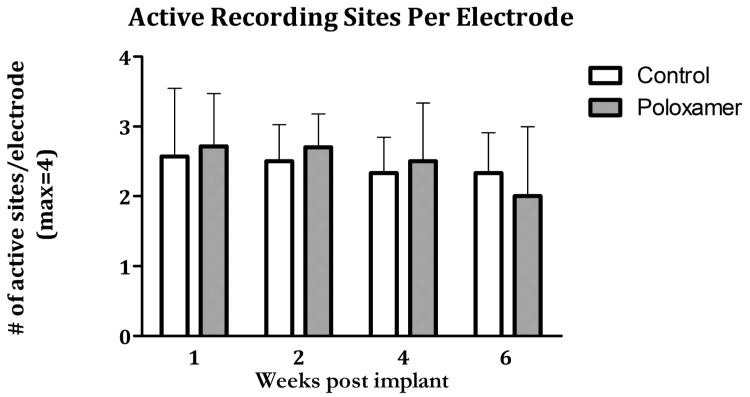

Figure 2.

Average number of active recording sites (sites where action potentials from 1 or more neuron was observed) in control and Poloxamer coated implants over the 6 week study period. No significant differences exist between coatings conditions or time points.

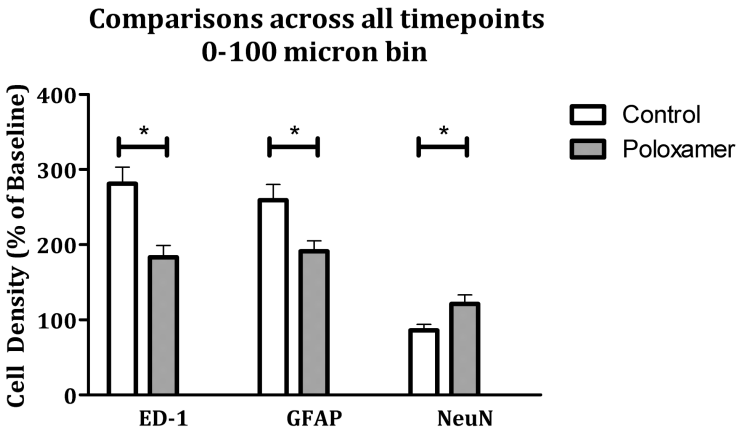

Figure 3.

Comparisons of cellular density in tissue found less than 100 microns away from the center of the implant across all time points. There is a pattern of significantly decreased immune reactivity and increased neuronal survival that is consistent across stains. Significance is set at the Bonferroni corrected p value of $p < 0.016$.

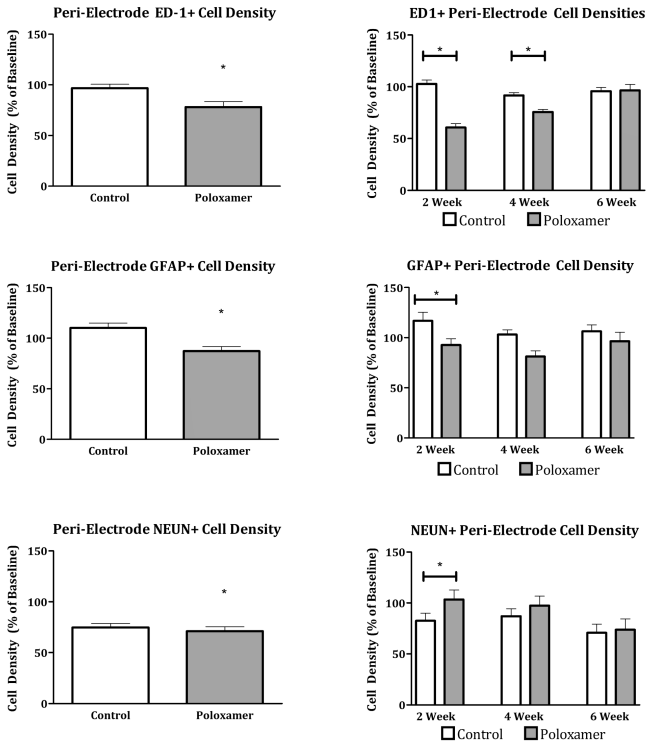

Figure 4.

Left) Average cell density of microglia (TOP), glia (MIDDLE), and neurons (BOTTOM) for control and Poloxamer groups. Significance is set at $p < 0.05$. Right) Planned comparisons between Poloxamer coated and control implants at 2, 4 and 6 weeks for microglia (TOP), glia (MIDDLE), and neurons (BOTTOM) Significance is set at the Bonferroni corrected value $p < 0.016$

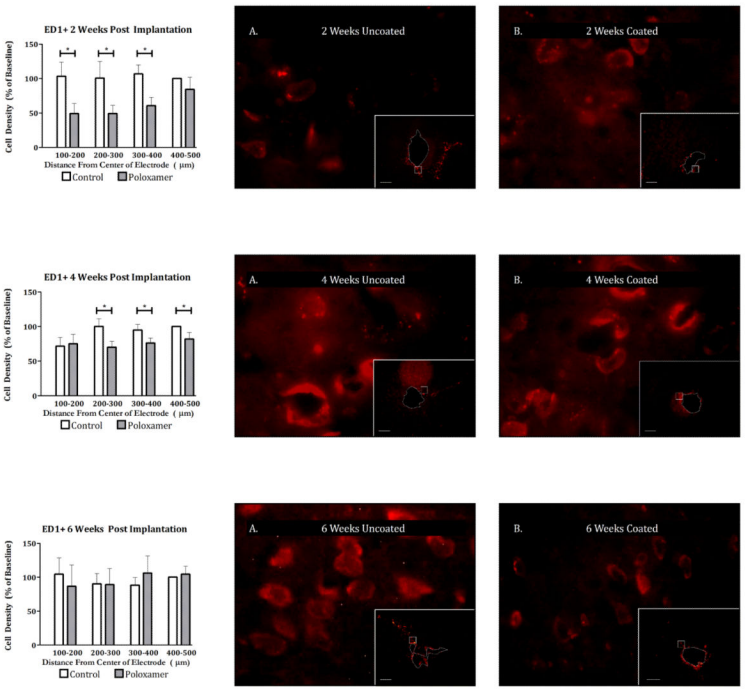

Figure 5.

Left) Planned comparisons between peri-electrode ED1 positive cell count in Poloxamer coated and control implants at 2 weeks (TOP), 4 weeks (MIDDLE), and 6 weeks (BOTTOM) post implantation. Significance is set at the Bonferroni corrected $p < 0.004$. Right) 100x Photomicrographs of exemplar peri-electrode tissue surrounding uncoated (A) versus Poloxamer coated (B) controls. Insets are 5x images of the entire implant site. The white dotted line represents the border of the explant site. Scale bar = 100um. Post processing adjustments for brightness and contrast are for publication purposes only. Data collection was done on the tissue directly.

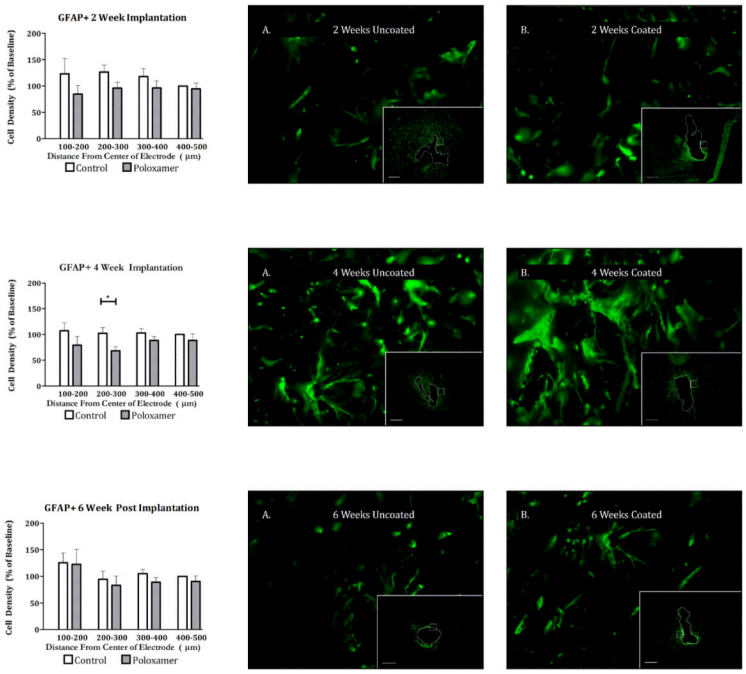

Figure 6.

Left) Planned comparisons between peri-electrode GFAP positive cell count in Poloxamer coated and control implants at 2 weeks (TOP), 4 weeks (MIDDLE), and 6 weeks (BOTTOM) post implantation. Significance is set at the Bonferroni corrected $p < 0.004$. Right) 100x Photomicrographs of exemplar peri-electrode tissue surrounding uncoated (A) versus Poloxamer coated (B) controls. Insets are 5x images of the entire implant site. The white dotted line represents the border of the explant site. Scale bar = 100um. Post processing adjustments for brightness and contrast are for publication purposes only. Data collection was done on the tissue directly.

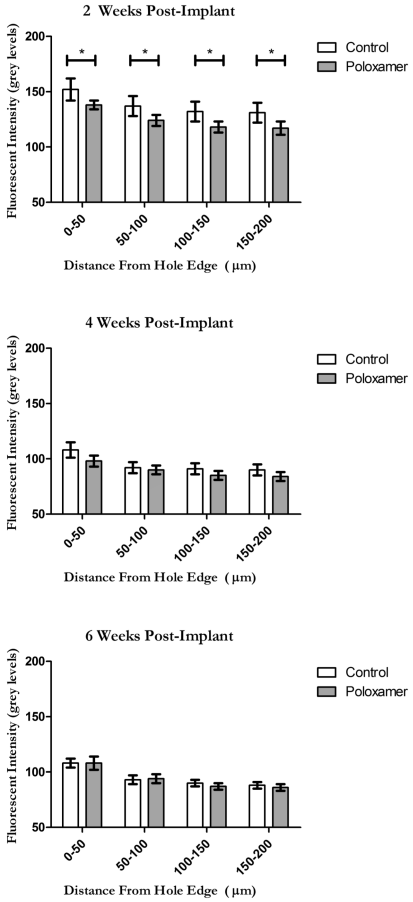

Figure 7.

GFAP fluorescent intensity profiles as measured from the edge of the explant site (Note that 0 is no longer the center of the hole as it was in the cell count analysis) at 2 weeks (TOP), 4 weeks (MIDDLE) and 6 weeks (BOTTOM). The y axis scale is reported in grey levels where 0 represents the grey level of normal tissue found far from the implant site. Significance is set at the Bonferroni corrected $p < 0.004$.

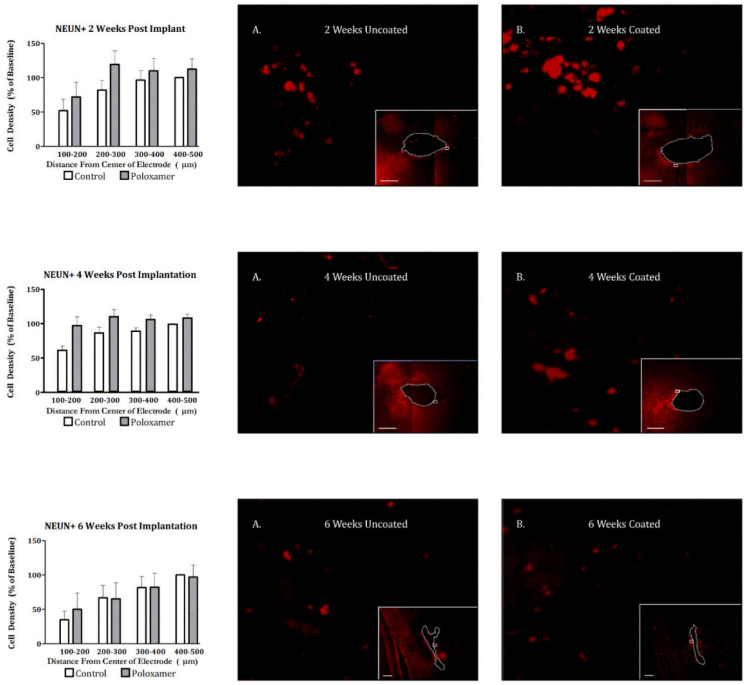

Figure 8.

Left) Planned comparisons between peri-electrode neuron count in Poloxamer coated and control implants at 2 weeks (TOP), 4 weeks (MIDDLE), and 6 weeks (BOTTOM) post implantation. Significance is set at the Bonferroni corrected $p < 0.004$. Right) 100x Photomicrographs of exemplar peri-electrode tissue surrounding uncoated (A) versus Poloxamer coated (B) controls at 2 weeks (TOP), 4 weeks (MIDDLE), and 6 weeks (BOTTOM) post implantation. Insets are 5x images of the entire implant site. The white dotted line represents the border of the explant site. Scale bar = 100um. Post processing adjustments for brightness and contrast are for publication purposes only. Data collection was done on the tissue directly.